Characterization of Thin Liquid Films Using Molecular Dynamics Simulation

Jaeil Lee, Seungho Park*, Ohmyoung Kwon
Department of Mechanical and System Design Engineering, Hongik University, Seoul 121-791, Korea
Young Ki Choi
School of Mechanical Engineering, Chung-Ang University, Seoul 156-756, Korea
Joon Sik Lee
School of Mechanical and Aerospace Engineering, Seoul National University, Seoul 151-742, Korea

Various characteristics of a thin liquid film in its vapor-phase are investigated using the molecular dynamics technique. Local distributions of the temperature, density, normal and tangential pressure components, and stress are calculated for various film thicknesses and temperature levels. Distributions of local stresses change considerably with respect to film thicknesses, and interfacial regions on both sides of the film start to overlap with each other as the film becomes thinner. Integration of the local stresses, i.e., the surface tension, however, does not vary much regardless of the interfacial overlap. The minimum thickness of a liquid film before rupturing is estimated with respect to the calculation domain sizes and is compared with a simple theoretical relation.

Key Words : Thin Liquid Film, Surface Tension, Molecular Dynamics, Interfacial Overlap

Nomenclature

d_i : Interface thickness
F : Force
k_B : Boltzmann constant
L : Simulation domain size
m : Molecular mass
n : Number density
N : Total number of molecules
P : Pressure
r : Molecular position
r_c : Cutoff radius
r_{ij} : Inter-distance between molecules i and j
t : Time
T : Temperature
v : Velocity
z : Direction normal to the film
z_o : Parameter for a fitting function

Greek Symbols

γ : Surface tension
ε : Energy parameter
σ : Length parameter
Φ : Potential function

Superscript

$*$: Dimensionless

Subscripts

f : Film
I : Intermolecular
K : Kinetic
n : Normal
sl : Slab
t : Tangential
x,y,z : Directions in rectangular coordinate

* Corresponding Author,
E-mail : spark@hongik.ac.kr
TEL : +82-2-320-1632; **FAX** : +82-2-332-7003
Department of Mechanical and System Design Engineering, Hongik University, Seoul 121-791, Korea.
(Manuscript **Received** January 30, 2002; **Revised** July 15, 2002)

1. Introduction

Because of its critical importance in many scientific and engineering applications, various characteristics of a liquid thin film have been investigated for well over a century. Those applications include wetting phenomena, phase-change phenomena, material processing, lubrication, and so on. The importance of the interfacial regions and their characteristics has become more pronounced due to the development of micro-and nano-scale systems. The main reason is that the interfacial regions are not infinitesimally thin compared to other length-scale dimensions and their behavior governs the transport phenomena and mechanical properties in such small systems, which are considerably deviated from those for macroscopic systems (Abramson and Tien, 1999 ; Weng et al., 2000a).

Since thin film properties are extremely difficult to estimate experimentally, most studies rely on the theoretical and numerical analyses. One of the promising tools for investigating the microscopic phenomena is the molecular dynamics simulation : it can yield a detailed molecular motion in a time step of less than one femtosecond. Although the geometrical and the temporal scales in the simulation are quite limited owing to large computational efforts, microscale behavior of materials and their properties can be estimated by appropriate applications of molecular dynamics techniques (Allen and Tildesley, 1987 ; Haile, 1992).

After the work by Chapela et al. (1977) a number of investigations have been conducted on the liquid-vapor films by using molecular dynamics simulations. Nijmeijer et al. (1988) calculated surface tensions of a liquid film in its vapor-phase, although their local stress distributions turned out to be physically incorrect due to the oversimplification of pressure tensors. That limitation has been addressed by Weng et al. (2000b) and the resulting local stress distributions seemed to be physically valid. Hwang et al. (1988) observed the rupture process of a free liquid film and a film on a solid substrate. However, a detailed investigation of interfacial properties such as the local temperature, local density, local pressures, surface tension, and minimum thickness of films has not been carried out.

The object of the current study, therefore, is to explore the interfacial regions of liquid films and their characteristics in sufficient detail. In addition, the minimum thickness of films before rupturing is calculated and compared to a theoretical model derived from a simple stability analysis based on the minimum energy criterion (Weng et al., 2000b ; Majumdar and Mezic, 1998).

2. Simulation Model

The present study on the characteristics of thin liquid film utilizes the Lennard-Jones (LJ) 12-6 potential, given as

$$\Phi(r_{ij})=4\varepsilon\left[\left(\frac{\sigma}{r_{ij}}\right)^{12}-\left(\frac{\sigma}{r_{ij}}\right)^{6}\right] \tag{1}$$

where the length parameter $\sigma=0.34$ nm and the energy parameter $\varepsilon=1.67\times10^{-21}$ J. These parameters are based on argon whose molecular mass is $m=6.63\times10^{-26}$ kg. Here r_{ij} denotes the inter-distance between molecules i and j. The LJ potential is truncated to zero for distances larger than 3.0σ without long-range force corrections. A simulation domain of $L_x^*\times L_y^*\times L_z^*$ is schematically shown in Fig. 1, with periodic boundary conditions in all three directions.

The molecular motion is simulated by solving Newton's equation of motion with intermolecular forces obtained from Eq. (1),

$$F_i=-\sum_{j\neq i}^{n}\frac{\partial\Phi(r_{ij})}{\partial r_i}=m_i\frac{d^2r_i}{dt^2} \tag{2}$$

using the "velocity Verlet" algorithm (Swope, et al., 1982) with a time-step of 5 fs or $\Delta\tau^*=2.335\times10^{-3}$. In this work all quantities with an asterisk are nondimensionalized with respect to σ, ε, and m.

Before the simulation run is initiated, a crystalline fcc structure is designed and placed at the center of the computational domain for each simulation condition. The initial velocity of each molecule is estimated by either applying the Maxwell-Boltzmann distribution at a given tem-

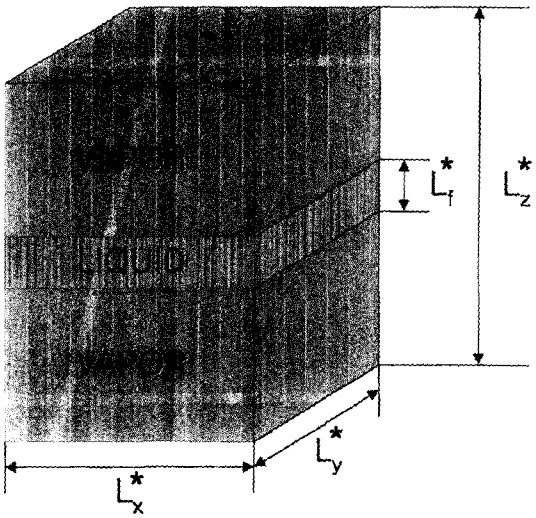

Fig. 1 System configuration for a thin liquid film in its vapor

perature or obtained from previous simulations, if available. The molecular system is equilibrated for more than 100,000 time-steps at the designed temperature using the velocity rescaling (Haile, 1992). This equilibration period is followed by the production period of 100,000 time-steps, in which the instantaneous values of the local density and stress are calculated at each time step. Time-averaged values are also calculated at the end of the production period. The local values are obtained in each thin slab of thickness $L_{sl}^*=0.1$ in the direction normal to the film surface (z direction in Fig. 1).

3. Results and Discussion

For the number of molecules $N=2500$ $T^*=0.818$ (99 K) in the domain of $L_x^*\times L_y^*\times L_z^*=17\times17\times58$, the temperature and density distributions are shown in Fig. 2(a). The local number density denotes the average number of molecules found in each slab divided by the slab volume, as given by

$$n^*=\left\langle\frac{N_{sl}}{V_{sl}^*}\right\rangle \tag{3}$$

and the local temperature is obtained from the kinetic energies of molecules existing in the slab, given by

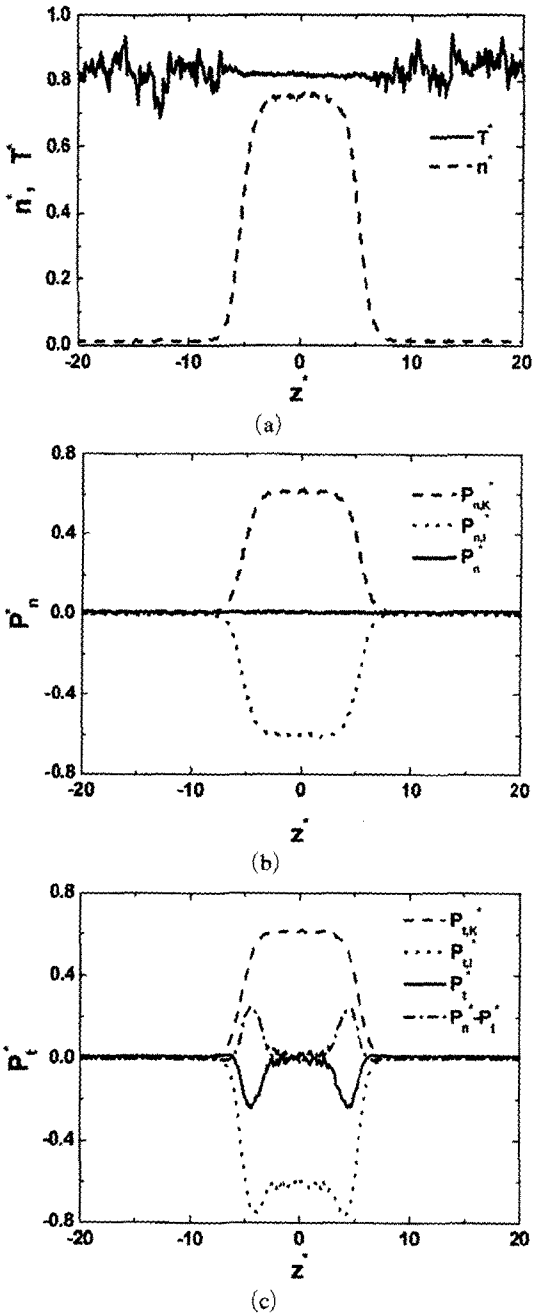

Fig. 2 Distributions of (a) temperature and density, (b) normal pressure, and (c) tangential pressure and local stress at 99 K (N=2500)

$$T^*=\frac{1}{3N_{sl}}\left\langle\sum_i^{N_{sl}} v_i^*\cdot v_i^*\right\rangle \tag{4}$$

where the angular brackets represent a time average. The density in the vapor-phase is about

0.01353, which is slightly higher than the experimental saturated vapor argon density (0.00925 at $T^*=0.818$) (Vargaftik, 1975). The density in the liquid-phase is about 0.7517, which is slightly lower than the experimental saturated liquid argon density (0.776 at the identical temperature). The temperature in the liquid-phase is well-behaved at about $T^*=0.818$, while that in vapor-phase fluctuates considerably around $T^*=0.818$. Figures 2(b) and (c) show the distributions of the normal and tangential components of pressures, which are obtained from the formulations given by,

$$P_n(k)=P_{n,K}-P_{n,I} =\langle n(k)\rangle k_B T -\frac{1}{V_{sl}}\left\langle \sum_{i,j}^{k}\left\{\frac{z_{ij}^2}{r_{ij}}\right\}\Phi'(r_{ij})f_{k,ij}\right\rangle \quad (5)$$

$$P_t(k)=P_{t,K}-P_{t,I} =\langle n(k)\rangle k_B T -\frac{1}{V_{sl}}\left\langle \sum_{i,j}^{k}\left\{\frac{\frac{1}{2}(x_{ij}^2+y_{ij}^2)}{r_{ij}}\right\}\Phi'(r_{ij})f_{k,ij}\right\rangle \quad (6)$$

where $n(k)$ is the number density in slab k and subscripts K and I denote the contributions from the kinetic motion of molecules and from the intermolecular forces, respectively. The parameter, $f_{k,ij}$, in $P_{n,I}$ and $P_{t,I}$ is defined as the ratio of the length that the force-line spans through slab k to the total length spun by the force-line (Weng, et al., 2000b). With these pressure components the surface tension (Rowlinson and Widom, 1982) can be expressed as

$$\gamma=\frac{1}{2}\int_0^{L_z}(P_n-P_t)\,dz \quad (7)$$

Figure 2(b) shows the kinetic ($P_{n,K}^*$) and intermolecular ($P_{n,I}^*$) contributions to the normal component of pressure tensor (P_n^*). In the vapor-phase region the intermolecular contribution is negligible compared to the kinetic contribution and thus, P_n^* becomes practically equal to its ideal gas pressure, which can be understood by Eq. (5). Although the absolute values of the contributions in the interfacial zone as well as in the liquid-phase region are much greater than those for the vapor-phase region, the differences between the two contributions are very close to its counterpart in the vapor-phase region, which implies the normal force balance across the interfacial region. On the other hand, the differences between the kinetic and intermolecular contributions to the tangential component, P_t^* become significant in the interfacial regions of the film, as shown in Fig. 2(c). The difference between P_n^* and P_t^* depicted by the dash-dot line engenders the surface tension of the film, using Eq. (7). It is clear that the interfacial stress is concentrated in the interface region between the liquid and vapor-phases.

Figures 3(a) and (b) show the effects of film thickness on the interfacial characteristics such as the local density and local stress distributions. For the cases of the molecular number exceeding 2500, the liquid and vapor-phases are clearly

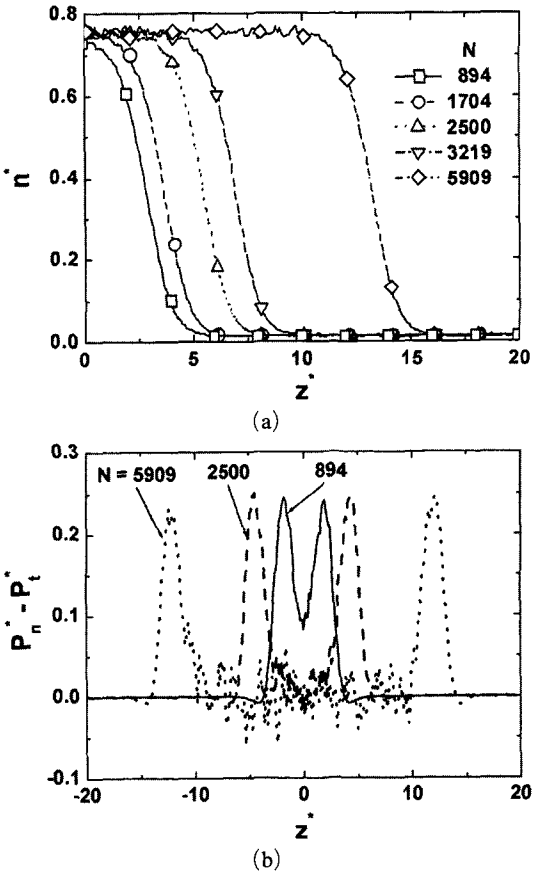

Fig. 3 Distributions of (a) density and (b) local stress for various thicknesses of thin liquid films at 99 K

Table 1 Characteristics of liquid thin films at 99 K

N	L_z^*	n_l^*	n_v^*	L_f^*	γ^*	d_i^*
894	40	0.7353	0.01422	5.6	0.5233	2.271
1704	47.88	0.7467	0.01393	7.2	0.5500	2.284
2500	57.38	0.7517	0.01353	10.3	0.5249	2.303
3129	57.38	0.7518	0.01373	13.4	0.5427	2.260
5909	71.38	0.7546	0.01408	25.7	0.5309	2.346

separated by the interfacial region shown in Fig. 3(a), while the liquid-phase regions for the cases of the molecular number less than 1704 are smeared into the interfacial region. These tendencies can be found in the local stress distributions shown in Fig. 3(b). For larger molecule number cases there exist stress-free regions in the liquid-phases that imply bulk-liquid-phase, while the local stresses on both sides of a film interact with each other and the stress-free regions disappear for smaller molecule number cases. Surfaces tensions for these cases, however, do not vary much as given in Table 1. The film thickness, L_f^*, in Table 1 is assumed to be the distance between equimolecular dividing surfaces on both sides of the film. In this simple geometry the equimolecular dividing surface is simply defined as the location of the local density having the average value of the liquid and vapor-phase densities,

$$n_{eq}^* = \frac{n_l^* + n_v^*}{2} \tag{8}$$

With the density distribution shown in Fig. 3 (a), the thicknesses of interfacial regions are estimated using the fitting function given by

$$n^*(z^*) = \frac{(n_l^* + n_v^*)}{2} - \frac{(n_l^* - n_v^*)}{2} \tanh\left[\frac{2(z^* - z_o^*)}{d_i^*}\right] \tag{9}$$

and are compared in Table 1. In spite of the differences in the film thickness (L_f^*), the interfacial thicknesses (d_i^*) are very close to each other, which can be understood by the slopes of density variation across the interfacial region. The estimated values for the interfacial thicknesses imply that the interface is composed of about 3 molecular layers.

Across the film almost all the regions are under tension, but there are regions under compression near the outer edge of the interfacial regions. Such phenomena have been observed in the previous studies and thought to be a numerical error induced by oversimplification of pressure components (Nijmeijer, et al., 1988). However, Eqs. (5) and (6) that are pressure components modified by Weng, et al. (2000b) result in the similar behavior in the local stress distribution, and remains to be explained physically.

The density distributions of thin liquid films are described in Fig. 4 for various temperatures. As expected, the liquid-phase densities decrease with increasing temperature, while the gas-phase densities increase. In addition, the surface tensions decrease with increasing temperature, as shown in Fig. 5. The differences in the surface tension are negligible for different molecular number cases, which is explained in Table 1. The

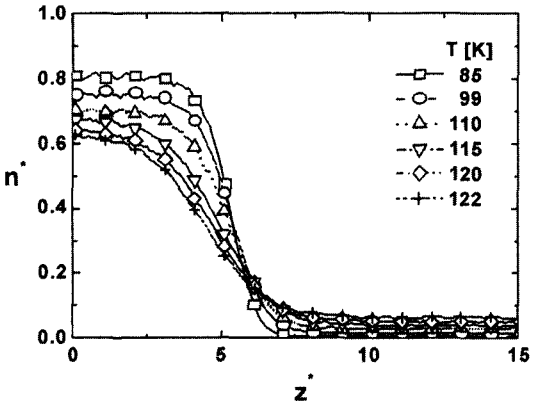

Fig. 4 Density distributions in thin liquid films with respect to temperatures (N=2500)

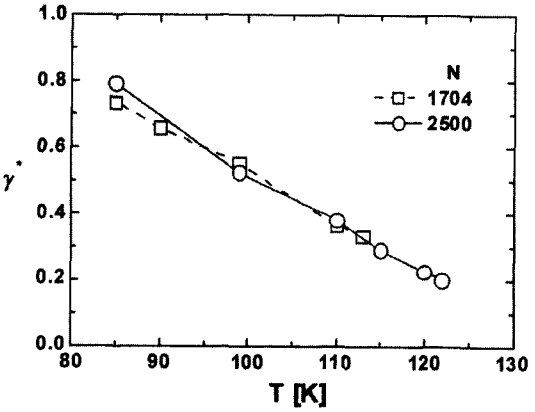

Fig. 5 Surface tensions for thin liquid films with respect to temperatures

effects of the cutoff radius, r_c, on film characteristics are shown in Figs. 6(a) and (b). While the differences between density distributions are insignificant for the cutoff radii greater than 3.0, the surface tensions vary considerably with the cutoff radii and their differences become smaller for the curoff radii greater than 5.0. This implies that the cutoff radii greater than 3. 0 are sufficient to observe molecular motions and distributions, while cutoff radii must be greater than 5.0 to effectively estimate force related properties. Shorter cutoff radii, however, are usually preferred in molecular dynamics simulations in spite of inherent inaccuracies, since computation time is proportional to $N_{rc}{}^{*2}$, where N_{rc}^* denotes the number of molecules inside the sphere formed by the cutoff radius.

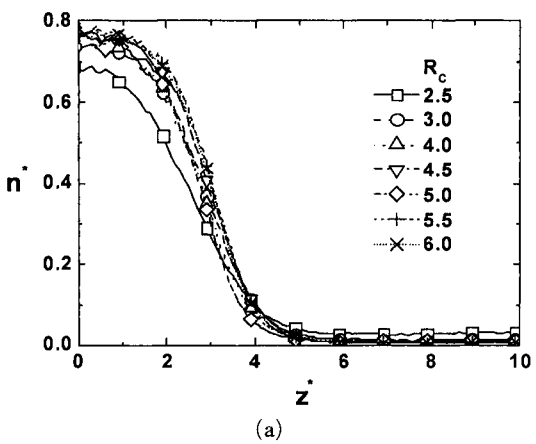

(a)

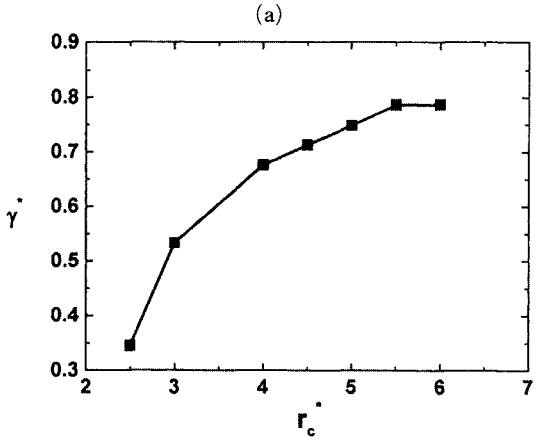

(b)

Fig. 6 (a) Density distributions and (b) surface tensions with respect to cutoff radii at 99 K

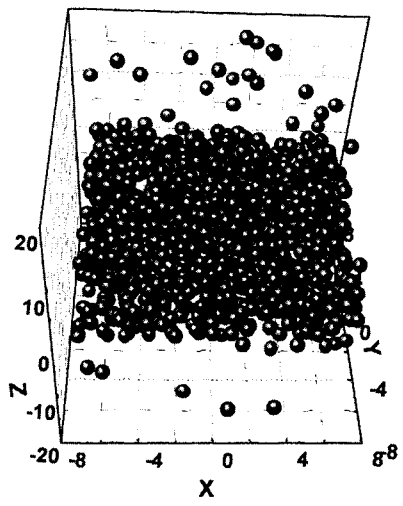

(a)

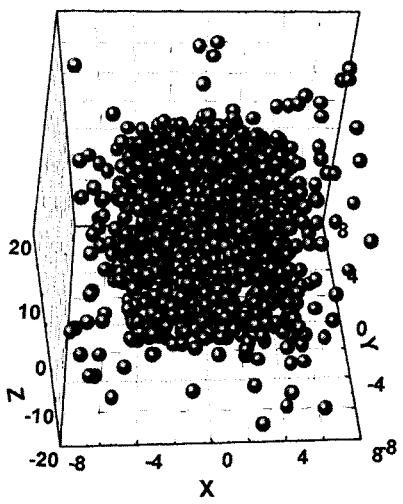

(b)

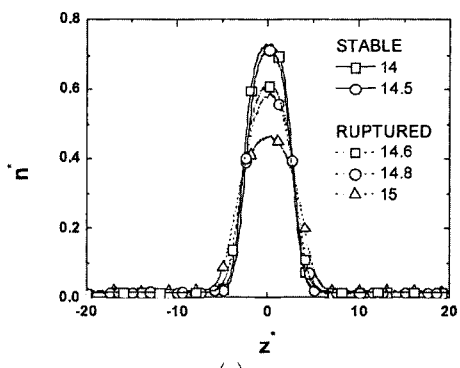

(c)

Fig. 7 Molecular and density distributions at 99 K (N=894): (a) stable liquid thin film with $L_x^*=14$, (b) ruptured film with $L_x^*=15$, and (c) local density distributions

One of the major advantages of molecular dynamics simulations is the capability to observe and to analyze critical phenomena occurring in a very small temporal and/or spatial-scales, which cannot be experimented even with a sophisticated apparatus. Among various critical phenomena, the rupture of a liquid film can be observed by increasing the calculation domain in the x and y directions and estimating the minimum thicknesses of the film. Figures 7(a) and (b) show the molecular distributions for the domains of $L_x^*=L_y^*=14$ and 15, respectively. For the domain of $L_x^*=L_y^*=14$, the molecules form a thin film, while the film is ruptured and starts to roll into a cylindrical shape for larger domains. This critical change can be detected in the local density distributions for various domain sizes, as shown in Fig. 7(c). The density distributions for domains smaller than $L_x^*=L_y^*14.5$ show that the densities in the center region of films are very close to that for the bulk liquid-phase given in Table 1, while the densities are reduced significantly for domains larger than $L_x^*=L_y^*=14.6$.

By observing the density distributions the minimum thickness of the liquid film can be obtained with respect to the domain size and compared with a theoretical model given in Fig. 8. A simple stability analysis by Weng et al. (2000b) predicts that disturbances with the wavelengths smaller than the critical length, $\lambda_{cr}=L_f^2\sqrt{4\pi^3\gamma/A}$ cannot break the film and implies that the film may become unstable if $\lambda_{cr}<L_x$. Here, L_f is the film thickness and A is the Hamaker constant (Israelachvili, 1992). This stability criterion implies that the minimum film thickness is proportional to the maximum wavelength of disturbance and thus,

$$L_{f,\min}^* \propto \sqrt{L_x^*} \tag{10}$$

In general, the minimum film thickness estimated from the molecular dynamics simulation decreases as the domain size decreases, following the relation of Eq. (10). However, more rigorous investigations are corroborated to estimate the simple relation thoroughly, since the calculation domain spans only a very small range of film sizes. In addition, the limit of the minimum film thickness with the decrease of domain sizes is another topic for future study, since the smallest thickness of the film in Fig. 8 is already close to the depth for only three layers of fcc argon structure.

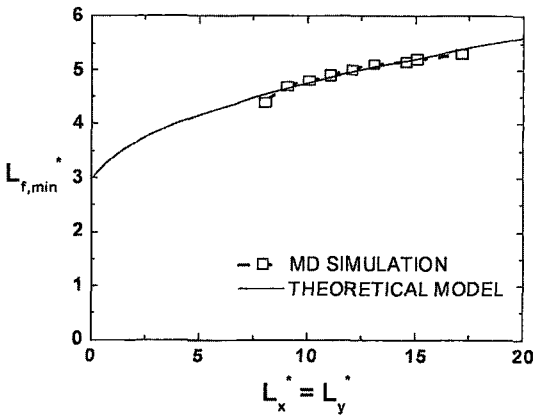

Fig. 8 Critical film thicknesses with respect to domain sizes

4. Conclusions

This study reports on various characteristics of thin liquid films that have been derived through molecular dynamics simulations. The main conclusions are as follows.

Surface tensions do not change with film thicknesses, although distributions of local stresses change considerably. For films of large thickness there exists a stress-free region between both sides of interfaces, while the region disappears for films of smaller thickness and the interfacial regions on both sides of the film start to overlap.

As expected from conventional experiments, the density in the liquid-phase region and surface tension decrease with increasing temperature, while density in the gas-phase region increases slightly. For the cutoff radii greater than 3.0, the differences between density distributions are not significant, while the differences between surface tensions become smaller for the cutoff radii greater than 5.0.

Based on the density distribution, the minimum thickness of a liquid film is estimated and compared with a simple theoretical relation. Within

the span of the domain sizes adopted in the current investigation the results agree with the theoretical model.

Acknowledgment

The authors gratefully acknowledge financial support from the Micro Thermal System Research Center sponsored by the Korea Science and Engineering Foundation and S. H. Park has been partially supported from the Basic Research Program of the Korea Science & Engineering Foundation under grant No. 1999-1-304-002-5.

References

Abramson, A. R. and Tien, C. L., 1999, "Recent Developments in Microscale Thermophysical Engineering," *Microscale Thermophysical Engineering*, Vol. 3, pp. 229~244.

Allen, M. P. and Tildesley, D. L., 1987, *Computer Simulation of Liquids*, Oxford University Press, New York.

Chapela, G. A., Saville, G., Thompson, S. M. and Rowlinson, J. S., 1977, "Computer Simulation of a Gas-Liquid Surface," J. Chem. Soc. Faraday Trans. II, Vol. 73, p. 1133.

Haile, J. M., 1992, *Molecular Dynamics Simulation*, John Wiley & Sons, pp. 260~267.

Hwang, C. C., Hsieh, J. Y., Chang, K. H. and Liao, J. J., 1988, "A Study of Rupture Process of Thin Liquid Films by a Molecular Dynamics Simulation," Physica A 256, pp. 333~341.

Israelachvili, J., 1992, *Intermolecular and Surface Forces*, Academic, London, pp. 176~212.

Majumdar, A. and Mezic, I., 1998, "Stability Regimes of Thin Liquid Films," *Microscale Thermophysical Engineering*, Vol. 2, pp. 203~213.

Nijmeijer, M. J. P., Bakker, A. F., Bruin, C. and Sikkenk, J. H., 1988, "A Molecular Dynamics Simulation of the Lennard-Jones Liquid-Vapor Interface," *Journal of Chemical Physics*, Vol. 89, pp. 3789~3792.

Rowlinson, J. S. and Widom, B., 1982, *Molecular Theory of Capillary*, Clarendon, Oxford, pp. 69~128.

Swope, W. C., Anderson, H. C., Berens, P. H. and Wilson, K. R., 1982, "A Computer Simulation Method for the Calculation of Equilibrium Constants for the Formation of Physical Clusters of Molecules: Application to Small Water Clusters," *Journal of Chemical Physics*, Vol. 76, pp. 637~649.

Vargaftik, N. B., 1975, *Table on the Thermophysical Properties of Liquids and Gases*, Hemisphere, Washington, D. C., p. 543.

Weng, J. G., Park, S. H. and Tien, C. L., 2000a, "Interfacial Ambiguities in Microdroplets and Microbubbles," *Microscale Thermophysical Engineering*, Vol. 4, pp. 83~87.

Weng, J. G., Park, S. H., Lukes, J. R. and Tien, C. L., 2000b, "Molecular Dynamics Investigation of Thickness Effect on Liquid Films," *Journal of Chemical Physics*, Vol. 113, pp. 5917~ 5923.